

1
2
3
4
5
6
7
8
9
10
11
12
13
14
15
16
17
18
19
20

Solid state characterization and effect of PEG 20000 and lecithin on particle size reduction and stability of complexed glibenclamide nanocrystals

ABSTRACT

Aims: To formulate and characterize GLB-PEG-LEC NCs (lecithin complexed Glibenclamide nanocrystals) and to analyze the effect of PEG 20000 and lecithin on drug properties, particle size reduction and stability of GLB NCs.

Study Design: Precipitated (GLB-PEG) and complexed nanocrystals (GLB-PEG-LEC) of glibenclamide were characterized for particle size, size distribution, zeta potential and stability assessment using photon correlation spectroscopy. The crystallinity, compatibility and surface morphology were analyzed using differential scanning calorimetry, powder x-ray spectroscopy, infrared spectroscopy and scanning electron microscopy.

Place and Duration of study: Asian Institute of Medicine Science and Technology, Malaysia, between May 2102 and June 2013.

Methodology: GLB-PEG NCs were prepared by precipitation technique using PEG 20000 and complexed by soybean lecithin. The effect of lecithin in particle size reduction, change in crystallinity, stability and surface properties of NCs were analyzed and compared with pure glibenclamide (GLB) and precipitated NCs. The formulations were optimized and its stability was also assessed for a 3 month period.

21 **Results:** Pure GLB exhibited an average particle size of 1551 nm. The average particle size of
22 precipitated NCs was between 236 - 7000 nm, while that of complexed NCs was between 155 -
23 842 nm. The particle size of NC was found to decrease, whereas its zeta potential was found to
24 increase after complexation. DSC studies showed no change in crystalline structure. PXRD
25 studies proved that crystallinity was maintained in NCs. SEM analysis showed spherical shape
26 particles resembling micelles after complexation. Stability studies revealed no change in particle
27 size during 3 month period. FTIR studies showed the compatability of excipients with the drug.

28

29 **Conclusion:** These results show that lecithin complexed GLB NCs could be utilized as
30 promising carriers for drug delivery due to its high stability and lower particle size.

31 **Keywords:** *Nanocrystals, complexation, lecithin, stability, particle size, precipitation*

32

33 **List of Abbreviations**

34 NCs: Nanocrystals

35 NPs: Nanoparticles

36 GLB: Glibenclamide

37 PEG: Polyethylene glycol

38 LEC: Lecithin

39 PDI: Polydispersity index

40

41

42 1. INTRODUCTION

43 Nanotechnology has emerged as a pivotal area of research and it may affect our lives
44 tremendously over the next decade in every field, including medicine and pharmacy [1]. In
45 medicine and pharmaceuticals, nanotechnology is used to improve human health at molecular level
46 and is applied in development of nanoparticulate systems [2]. Although a number of
47 nanoformulations are available and clinically approved in the past decade, its limitations like
48 comprehensive structure-function relationships between particle structure and its
49 pharmacological properties inhibit their wide spread adoption [3]. The size, shape, composition,
50 surface properties of nanocarriers, effects on pharmacokinetics and pharmacodynamics profiles
51 need to be clearly elucidated. These characterizations are emerging as new focus for assessing
52 the safety and efficiency of various nanoformulations [4].

53 The drug delivery efficiency of a nanoformulation depends on variety of factors like the
54 type of formulation, particle size, surface properties and stability of particles in medium. Ideally
55 a successful nanoformulation should have high drug loading capacity, considerable drug release,
56 and polymer degradation [5].

57 Nanoformulations include nanocrystals, carbon nanotubes, fullerenes, polymeric
58 micelles, nanosuspensions and nanoemulsions, and they are generally prepared by top down or
59 bottom up approach [6]. Compared to all nanoformulations, nanocrystals are considered to be the
60 least complex and are developed by precipitation or nanonization process. Nanocrystals (NCs)
61 contain 100% drug with no carriers, offer excellent solubility and can solve the issues associated
62 with poor solubility of a drug [7]. Nanonization or nanosizing techniques reduce the particle size
63 and increase the surface area-to volume ratio of drugs thereby offering higher rate of drug

64 dissolution [8]. The particle size reduction process of NCs depends upon the type of polymers,
65 surfactants, stabilizers and the milling method [9].

66 NCs possess major limitations like crystal growth (aggregation) on contact with fluids or
67 electrolytes, and loss in its functional properties [10]. A strategy to overcome the limitations is to
68 increase the surface properties of NCs by attaching ligands to them or by increasing its
69 stealthiness by complexation [11]. This approach could decrease particle aggregation, improve *in*
70 *vivo* stability and could provide a more complete and consistent absorption profiles similar to
71 solid lipid nanoparticles (SLN) [12].

72 During the production process of NCs, real time monitoring of immediate NCs and
73 assurance tests for final product are necessary. This could help in development of a stable
74 formulation and the drugs could be delivered safely and efficiently at a particular site with
75 improved bioavailability. Solid state characterization could provide useful information about the
76 properties of NCs. Parameters like particle size, zeta potential, size distribution, surface
77 morphology, crystallinity and aggregation need to be controlled precisely as they may affect the
78 ADME and toxicity of nanoformulation [13]. The above properties can be analyzed using Photon
79 Correlation Spectroscopy, Powder X-ray Diffractometry (PXRD), Differential Scanning
80 Calorimetry (DSC), Infrared Spectroscopy (FTIR) and Scanning Electron Microscope (SEM).

81 GLB is a second generation oral hypoglycemic agent (BCS Class II drug), with high
82 permeability, low aqueous solubility ($\sim 38 \mu\text{mol L}^{-1}$ at 37°C) and poor dissolution rate [14,15].
83 GLB is also a drug of choice for long term therapy for diabetes mellitus and it requires a rapid GI
84 absorption, to prevent a sudden increase in the blood glucose level after food intake [16]. The
85 objective of the present study is to formulate and characterize the properties of Glibenclamide

86 NCs (GLB) by various techniques. NCs were developed by precipitation process using PEG
87 20000 and stabilized (complexed) by means of soybean lecithin. The effect of PEG 20000 and
88 lecithin on particle size reduction and change in crystallinity of NCs were also assessed. Solid
89 state characterization studies facilitate in development of a stable formulation with fewer drugs -
90 excipient interactions and enable to design a formulation with improved therapeutic efficiency.

91 **2. MATERIALS and METHODS**

92 *2.1 Materials*

93 Glibenclamide sample was obtained from S.D Biomed (Malaysia). PEG 20000 and
94 soybean lecithin was procured from Sigma Aldrich, Malaysia. Acetone, Tween 80, sodium
95 dodecyl sulphate, polysorbate 80, dichloromethane and methanol were purchased from R and M
96 Chemicals, (Malaysia). Deionized water was obtained from Millipore, MilliQ-Plus. All the other
97 solvents and reagents used were of Anala R grade.

98

99 *2.2 Methods*

100 *2.2.1 Preparation of GLB-PEG NCs*

101 GLB was dissolved in a solvent mixture of acetone and methanol (2:1). PEG 20000 was
102 added to the drug solution and stirred at a temperature not exceeding 60°C. The drug-polymer
103 solution was injected slowly into an aqueous phase containing Tween 80 (3% w/v) as stabilizer
104 with mechanical stirring (400 rpm) overnight at room temperature to precipitate NCs. The
105 volume of dispersion was adjusted to 100 ml using double distilled water. The solution was then
106 gently heated with magnetic stirring for 30 min to remove the organic solvent. Later, the contents
107 were centrifuged (5000 rpm) for 20 min to separate the NCs. The clear supernatant liquid was
108 discarded, and the thick viscous dispersion was collected and further redispersed in 15 ml of

109 distilled water and recentrifuged (20000 rpm) for 10 min to remove the impurities and the
110 residual surfactants. The NCs were recovered using a vacuum filter (0.2 μm) and dried in a hot
111 air oven at 35°C for 20 min. The procedure was repeated to prepare different batches [17].

112

113 *2.2.2 Complexation of GLB-PEG NCs*

114 GLB-PEG NCs were complexed using soybean lecithin. 50 mg of dried NCs were
115 accurately weighed and dispersed in 50 ml of phosphate buffer (pH 7.4) in presence of 0.1 % w/v
116 Tween 80 by gentle stirring for 10 min. Soybean lecithin (2% w/v) previously solubilized in
117 chloroform was gradually added to the dispersion and stirred continuously using a magnetic
118 stirrer at 250 rpm for 30 min at a temperature above its melting point so as to obtain a
119 homogenous dispersion. The dispersion was transferred to a shaking incubator at 120 rpm for 1 h
120 at 15°C. Later, 5% w/v mannitol was added to the dispersion and shaken for 10 min prior to
121 lyophilization [18].

122

123 *2.2.3 Freeze Drying*

124 The milky homogenous dispersion was subjected to freeze drying in a freeze dryer
125 (Thermo Scientific, USA), with an inbuilt Pirani 501 microprocessor. The samples were
126 lyophilized at a slow freezing temperature (shelf temperature -40 °C at 6 torr and 10^{-1} m bar
127 pressure) for 10 h. The lyophilized products were stored in borosilicate glass vials and placed in
128 a dessicator until further use.

129

130 *2.4 Solid State Characterization*

131 *2.4.1 Photon Correlation Spectroscopy (PCS)*

132 The mean particle size and polydispersity index (PDI) of precipitated and complexed NCs
133 were measured using Malvern Zetasizer Nano ZS (Malvern Instruments, UK). 2 mg of NC was
134 dispersed in 150 ml of deionized water containing 0.1% w/v of tween 80 and 0.15 mg of sodium
135 dodecyl sulphate (SDS). The dispersion was sonicated using a bath sonicator (Power sonic 410,
136 Lab Tech, Korea) and kept aside for 24 h prior to analysis. 4 μ l of each suspension was diluted
137 with 2 ml of deionized water and the samples were pipetted into a disposable polystyrene
138 cuvette. The optimum volume was considered by positioning the cell to a marker line, drawn on
139 to the instrument panel. The samples were measured for the mean particle size and PDI at a fixed
140 angle of 90° and at a temperature of 25°C after 5 runs. A refractive index of 1.616 and 1.300
141 were used for the drug and solvent respectively [19].

142

143 *2.4.2 Zeta potential measurement (ZP)*

144 The zeta potential of precipitated and complexed NCs were measured using the light
145 scattering technique (M3-PALS) in a Malvern Zetasizer Nano ZS (Malvern Instruments, UK).
146 Samples were dispersed in deionized water and kept aside for 24 h and were injected into a clear
147 disposable zeta cell after suitable dilution. The zeta cell was checked for presence of air bubbles
148 and if any, was removed by tapping. The average zeta potential was measured after 3 scans.

149

150 *2.4.3 X-Ray Powder Diffraction (XRPD)*

151 XRPD diffractograms of pure GLB, polymers, physical mixtures (PM-1:1) and NCs
152 before and after complexation were recorded in X-ray diffractometer (Bruker AXS D8,
153 Germany) with Anton Paar, TTK 450 temperature attachment, using Si (Li) PSD detector. The

154 samples were placed in a glass sample holder and Cu ka radiation was generated at 30 mA and
155 40 Kv. The samples were scanned from 3° to 70° 2 θ with a step size of 0.02° [20].

156

157 *2.4.4 Differential Scanning Calorimetry (DSC)*

158 DSC analysis of pure GLB, polymer, physical mixtures (PM-1:1) and NCs before and
159 after complexation were analyzed in a DSC calorimeter (TA Instruments, Q200, USA), equipped
160 with a liquid nitrogen cooling system. About 5 mg of samples were loaded to aluminum pan,
161 crimped, sealed and further examined at a scanning rate of 10°C / min from 15 to 200°C under
162 nitrogen atmosphere (flow rate 100 ml/min) in room temperature. High purity indium was used
163 to calibrate the heat flow and heat capacity of the instruments [21].

164

165 *2.4.5 FTIR Analysis*

166 Spectra of pure GLB, PEG 20000, physical mixtures (PM-1:1) and NCs were recorded in
167 FT-IR spectrophotometer (Thermo Nicolet, Avatar 370, USA). The samples were compressed
168 into a pellet using KBr and scanned for 4 seconds at a resolution of 4 cm⁻¹ from 4000 to 400 cm⁻¹
169 [22].

170

171 *2.4.6 Scanning Electron Microscopy (SEM)*

172 Morphological evaluation of NCs was performed using a scanning electron microscope
173 (LEO 1530, Gemini, Germany). The samples were mounted to steel stubs (Jeol - 10 mm Dia x 5
174 mm) using a double sided adhesive tape and sputtered with a thin layer of Au at 20 mA, under
175 1x10⁻¹ bar vacuum for 10 min using a sputter coater (EM S550X - Electron microscopy sciences)
176 and was operated at an acceleration voltage of 3 kV [23].

177 *2.5 Stability Studies*

178 The optimized formulation (Batch F1) was placed in a clean airtight glass vials and stored
179 at room temperature and 37°C, RH = 75% over a period of 3 months. During the storage period,
180 the samples were evaluated for average particle size [24].

181

182 **3. RESULTS and DISCUSSION**

183 *3.1 Photon Correlation Spectroscopy*

184 *3.1.1 Effect of Polymer on Particle Size Reduction*

185 The particle size analysis data of precipitated and complexed NCs are shown in Table 1.
186 The average particle size of pure GLB was found to be 1551 nm, while that of precipitated NCs
187 (F1-F5) was between 236 - 7002 nm. The particle size was found to increase with an increase in
188 polymer content in precipitated NCs. The complexed NCs possessed an average particle size
189 between 155 nm and 842 nm and were found to decrease in all samples (F1 to F5).

190 The particle size distribution of precipitated NCs was found to be broader, while that of
191 complexed NCs were narrow as the PDI was below 0.5. It can be inferred that maximum size
192 reduction was observed in batch F1 with a drug- polymer ratio of 1:1.

193

194 *3.1.2 Effect of Zeta Potential and Stability of NCs*

195 The zeta potential of pure GLB, precipitated and complexed NCs are compared Table 1.
196 The zeta potential of precipitated NCs were much lower in comparison to pure GLB (-38.1 mV).
197 A high negative zeta potential value was observed in all samples after complexation by lecithin.
198 The stability of NCs is related to the charge imparted by lecithin that makes the drug particle get
199 disassociated within the system. The presence of high negative charge may be correlated to the

200 existence of number of carboxyl groups on the polymeric chain extremities and formation of a
 201 barrier between the particle surface and surrounding medium [25, 26].

202 **Table 1. Particle size and zeta potential report of GLB NCs.**

Batch	Drug : polymer	Precipitated NCs			Complexed NCs		
		Z.avg (d.nm)	PDI (avg.)	Avg. ZP (mV)	Z.avg (d.nm)	PDI (avg.)	Avg. ZP (mV)
Pure GLB	1:0	1551	0.417	-38.1 ± 0.2	-	-	-
F1	1:1	236	0.369	-35.1 ± 0.4	155	0.310	-51.7 ± 0.1
F2	1:2	5745	0.610	-29.0 ± 0.8	710	0.309	-45.8 ± 1.3
F3	1:4	7002	0.417	-34.3 ± 0.3	842	0.397	-48.4 ± 0.7
F4	1:8	5885	0.520	-32.3 ± 0.4	227	0.431	-58.3 ± 0.5
F5	2:1	3574	0.957	-20.2 ± 1.1	787	0.878	-48.0 ± 0.3

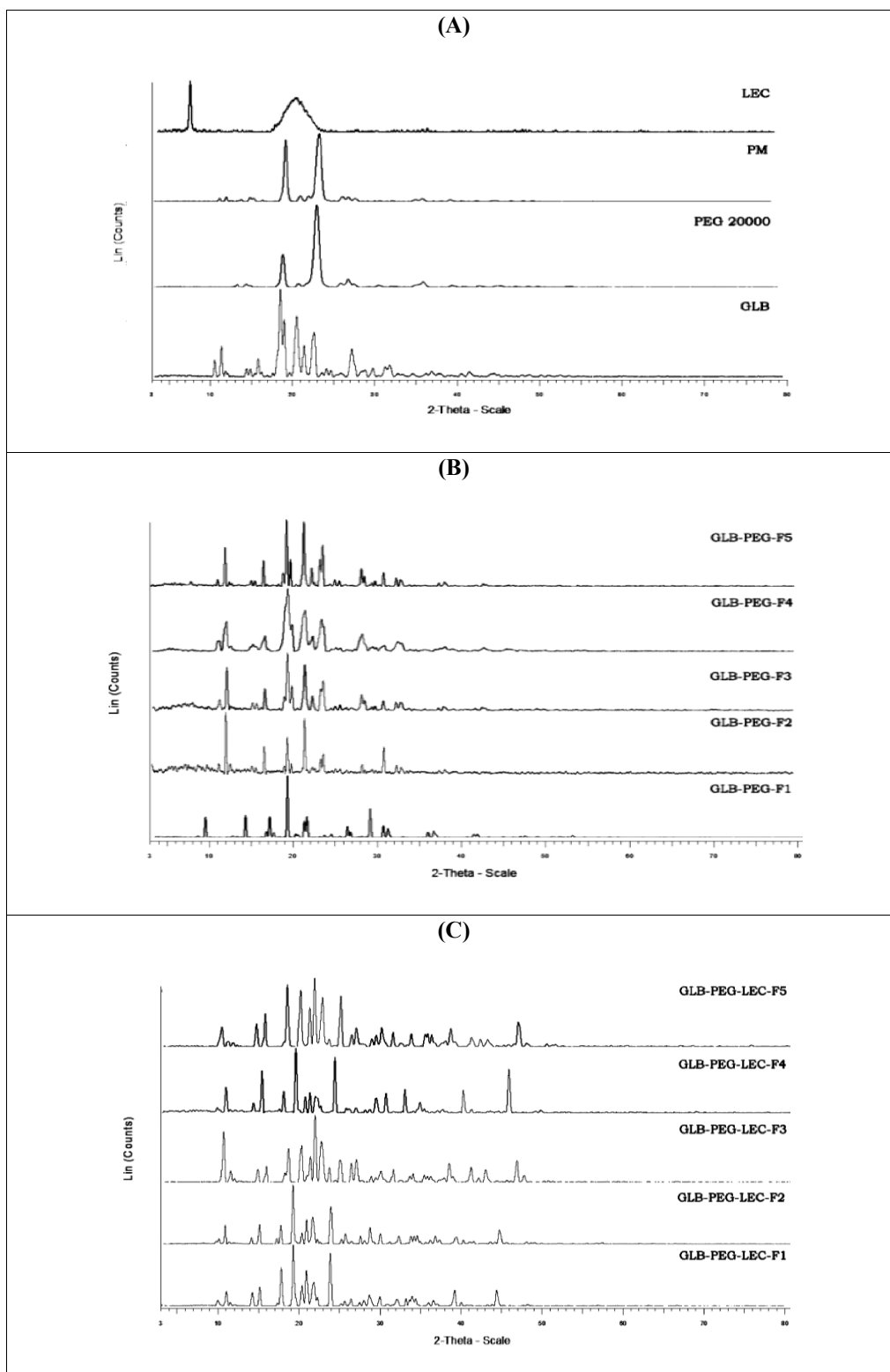
± indicates SD (n=3)

203

204 3.2 X-Ray Powder Diffraction

205 The diffraction spectra of pure GLB, physical mixture (PM-1:1), precipitated and
 206 complexed NCs are compared in Fig.1A, 1B and 1C respectively. The peak parameters like
 207 position, intensity and full width half maximum (FWHM) of NCs are shown in Table 2. Pure
 208 GLB spectra showed numerous sharp and narrow intense peaks at 2θ position like 10.85°,
 209 11.65°, 14.696°, 16.09°, 18.82°, 20.84°, 22.92°, 24.42°, 26.19°, 27.52°, 29.11° and 30.08°, and
 210 these observations prove its high crystalline nature. It was observed that all NCs exhibited a
 211 similar characteristic diffraction pattern as that of pure GLB specifically at 11.66°, 20.82° and
 212 30.08° 2θ positions revealing the absence of interaction between drug and polymer. Moreover,
 213 the intensity of the peaks was also slightly reduced in precipitated and complexed NCs. It was

214 also noticed the base of the peak was broadened, sharpness was found to decrease and peak area
215 lowered with increase in polymer content in samples. The relative intensity values (d-value)
216 decreased initially and became constant indicating that the crystallinity was maintained
217 irrespective of the polymer concentration and complexation. The presence of sharp and narrow
218 peaks in spectra of F5 proved the presence of high amount of drug.



219 **Fig.1. X-Ray Diffraction spectra of pure GLB, PEG 20000, PM (1:1) and Lecithin (A),**
220 **precipitated GLB NCs (F1-F5) (B), and GLB NCs (F1-F5) after complexation (C) at 2-**
221 **Theta-scale.**

222

223

224

225

226

227

228

229

230

231

232

233

234

235

236

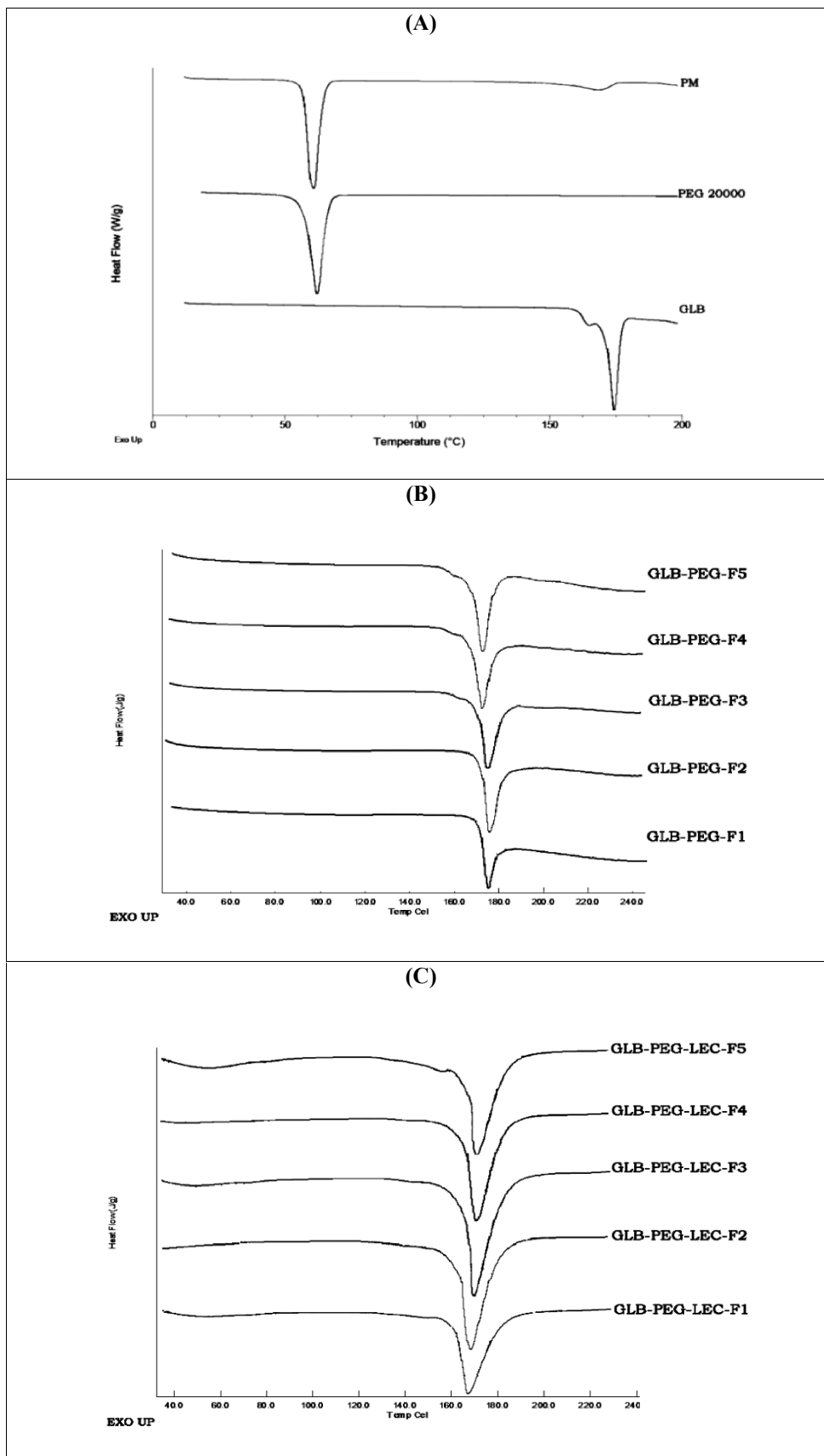
Table 2. XRPD peak parameters of GLB and formulations

Batch	Precipitated NCs			Complexed NCs		
	2 θ	Peak	FWHM	2 θ	Peak	FWHM
	position	intensity (d)	(deg)	position	intensity (d)	(deg)
Pure	11.66	7.58	-	-	-	-
GLB	20.82	4.26	0.46	-	-	-
	30.08	2.96	-	-	-	-
	11.80	7.49	0.19	10.71	8.24	0.22
F1	21.06	4.21	0.19	20.65	4.29	0.30
	30.37	2.94	0.20	30.62	2.91	-
	11.75	7.52	-	10.65	8.29	0.20
F2	21.03	4.22	0.19	21.35	4.15	0.37
	30.33	2.94	0.19	29.61	3.01	0.24
	11.82	7.47	0.23	10.75	8.21	-
F3	21.10	4.20	0.31	21.40	4.14	0.44
	30.42	2.93	-	30.66	2.91	-
	11.84	7.46	-	10.56	8.36	0.24
F4	21.07	4.21	-	20.56	4.31	0.23
	30.38	2.93	-	29.62	3.0	0.26
	11.82	7.48	0.19	11.22	7.87	-
F5	21.08	4.21	0.22	21.54	4.12	0.36
	30.38	2.93	-	29.70	3.00	0.24

FWHM-Full Width Half Maximum

239 *3.3 Differential Scanning Calorimetry*

240 DSC thermograms of GLB, PEG 20000, physical mixture (PM-1:1), precipitated and
241 complexed NCs are compared in Fig. 2A, 2B and 2C respectively. A sharp endothermic peak at
242 173.36°C ($\Delta H = 98.34$ J/g) in pure GLB thermogram indicated its high crystallinity and a broad
243 endothermic peak at 65.24°C in thermogram of PEG 20000 revealed its amorphous nature. Two
244 endothermic peaks (65.68°C and 164.61°C) observed in the thermogram of physical mixture
245 (1:1) proves the absence of interaction between drug and polymer. The glass transition
246 temperature (T_g) of endothermic peaks of precipitated NCs were found to be similar to pure
247 GLB indicating that there was no change in crystalline structure. The glass transition temperature
248 of complexed NCs showed a narrow change in peak (Fig.2C), indicating crystallinity was
249 maintained but with reduced size.



250 **Fig.2. DSC thermograms of Pure GLB, PEG 20000 and PM-1:1 (A), precipitated GLB NCs**
251 **(F1-F5) (B), and GLB NCs (F1-F5) after complexation (C).**

252

253 *3.4 FT-IR Analysis*

254 FT-IR spectra of pure GLB, PEG 20000, physical mixture (PM-1:1) and precipitated NCs
255 are compared in Fig.3A and 3B respectively. Pure GLB showed an obvious band at 1715.55 cm^{-1}
256 (carbonyl stretching), two characteristic bands at 1155.96 and 1306.29 cm^{-1} (symmetrical and
257 asymmetrical sulphonyl stretching) and bands at 3315.74 and 3367.82 cm^{-1} (amide stretching)
258 [27]. The presence of characteristic peaks of GLB in all formulations proved the compatibility
259 between drug and polymer.

260

261

262

263

264

265

266

267

268

269

270

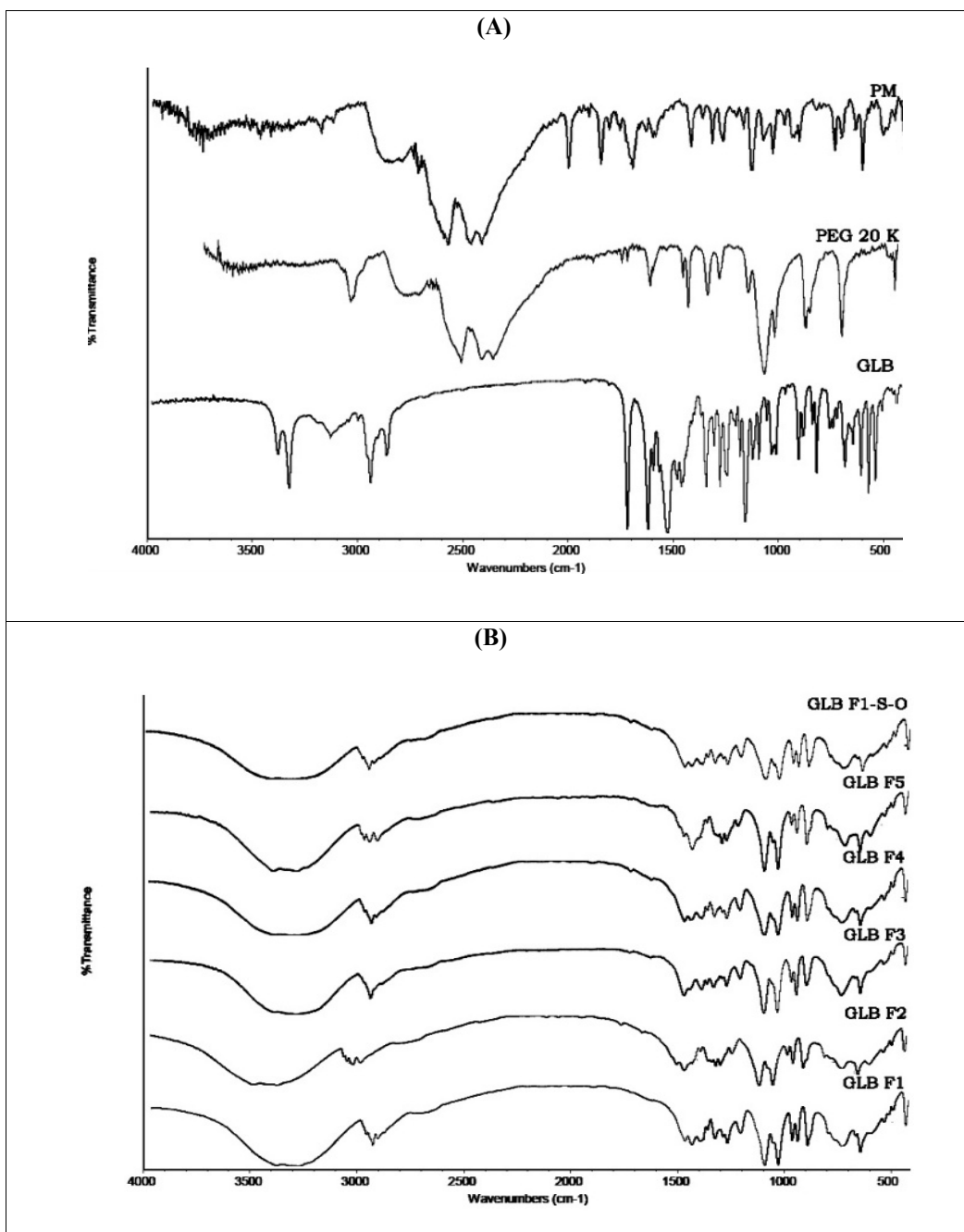
271

272

273

274

275



276

277

278

279

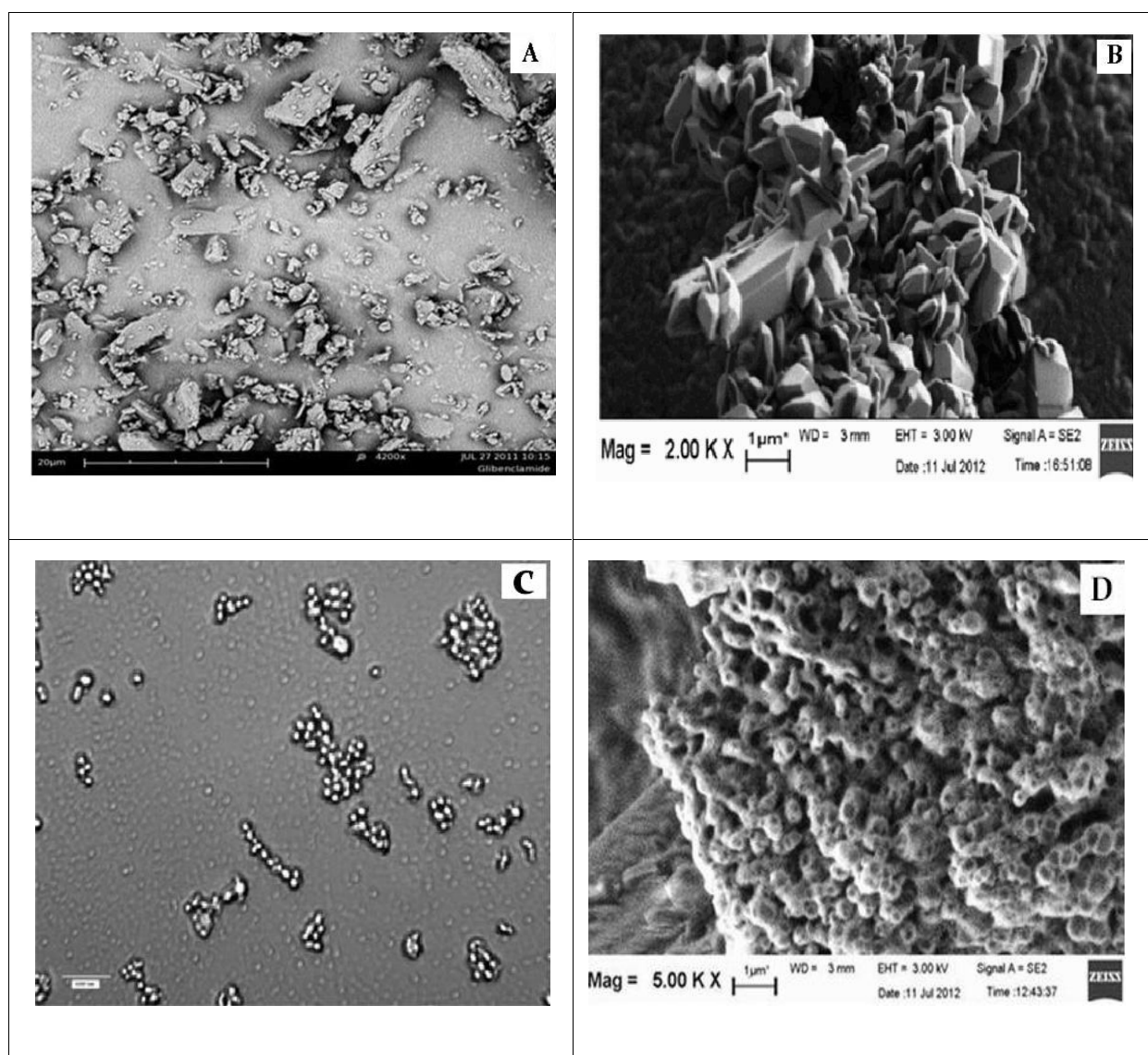
280

281

Fig.3. FTIR spectra of pure GLB, PEG 20000 and PM-1:1 (A), and precipitated GLB NCs (F1-F5) and optimized formulation (GLB- F1-S-O) after 3 months of storage (B).

282 3.5 Surface Characteristic Analysis

283 The SEM images of pure GLB (Fig.4A) showed numerous irregular shape particles with
284 large size ($>1.5 \mu\text{m}$), whereas precipitated NCs showed uniform prismatic crystals in an
285 agglomerated form with reduced size (Fig.4B). Fig.4C shows aggregated NCs after
286 microscopical examination. Fig.4D shows complexed NCs resembling micelles of smaller size
287 compared to precipitated NCs. A distinct difference in surface morphology was clearly observed
288 between precipitated and complexed NCs. The appearance of a waxy lipid layer on to the surface
289 of complexed NCs showed the presence of lecithin coating.



290 **Fig.4. SEM images of pure GLB (A), precipitated F1 NCs (B), aggregated NCs before**
 291 **complexation and after microscopical examination (C) and complexed F1 NCs (D).**

292

293 *3.6 Stability Analysis*

294 The stability data of optimized batch (F1) is given in Table 3. No significant change in
 295 particle size was observed during the storage period. The NCs were stable and less aggregated,
 296 and this stability of NCs could be due to the repulsive force associated with the molecules which
 297 reduce the particle agglomeration. Stability analysis of batch F1 was also studied using FTIR and
 298 the spectra was found to possess the characteristic peaks as of pure GLB at specific positions
 299 (GLB F1 SO, Fig.3B). These clearly prove that the chemical identity of GLB was preserved in
 300 the samples and the formulation was stable during the study period.

301

302 **Table 3. Stability data (Particle size analysis) of optimized batch (F1)**

Stability conditions	Observation (months)			
	0	1	2	3
Room Temperature	155	155	156	156
40°C (RH = 75%)	155	155	157	157

303

Values represent Z.avg (d.nm)

304

305 **4. CONCLUSION**

306 GLB NCs were formulated by precipitation technique and complexed using soybean
 307 lecithin. The solid state characterizations of NCs were performed and the factors were optimized.
 308 Batch F1 was found to be the optimum batch among the samples in terms of smaller particle size

309 and high stability. The particle size was found to decrease after complexation and was stable due
310 to high zeta potential. The crystallinity of GLB in NCs was not altered on treatment with PEG
311 20000 and after complexation. FTIR studies proved the absence of interaction between drug and
312 excipients. Stability studies show the NCs were stable for 3 months with no change in particle
313 size. These complexed NCs offer enhanced surface properties and could solve the stability issues
314 both *in vitro* and *in vivo*. They can be utilized as promising carriers for drug delivery due to its
315 high stability and lower particle size, and can also be effectively used in development of various
316 formulations.

317 **CONSENT and ETHICAL APPROVAL**

318 Not applicable

319

320 **COMPETING INTEREST**

321 The authors have declared that no competing interest exists.

322

323 **REFERENCES**

- 324 1. Jens UA, Rainer HM. Nanocrystal technology drug delivery and clinical applications. Int
325 J Nano Med. 2008; 3 (3): 295-99.
- 326 2. Tugba G, Gürsoy RN, Öner L. Nanocrystal technology for oral delivery of poorly water
327 soluble drugs. J Pharm Sci. 2009; 34 (1): 55-65.
- 328 3. Huabing C, Chalermchai K, Xiangliang Y, Xueling C, Jinming G. Nanonization
329 strategies for poorly water soluble drugs. Drug Discov Today. 2011; 16 (7-8): 354-60.
- 330 4. Banu SZ, Nakissa S. Regulatory perspective on the importance of ADME assessment of
331 nanoscale material containing drugs. Adv Drug Del Rev. 2009; 61 (6): 422-27.

- 332 5. Mohanraj VJ, Chen Y. Nanoparticles - A Review, Trop J Pharm Res. 2006; 5 (1): 561-73.
- 333 6. Marcato PD, Duran N. New aspects of nanopharmaceutical delivery systems. J Nanosci
334 Nanotech. 2008; 8 (5): 2216-29.
- 335 7. Rainer HM, Sven G, Cornelia MK. State of art nanocrystals - special features,
336 production, nanotoxicity aspects and intracellular delivery. Eur J Pharm Biopharm. 2011;
337 78 (1): 1-9.
- 338 8. Faris NB, Müller RH. Nanocrystals for poorly soluble drugs for oral administration.
339 Topics of PhD thesis and details on technologies, products, IP. New Drugs: 2002; 2 (2):
340 20-21.
- 341 9. Jaime S, Antoine G, Rainer HM, Jan PM. Nanocrystals: Comparison of the size reduction
342 effectiveness of a novel combinative method with conventional top-down approaches.
343 Eur J Pharm Biopharm. 2012; 81 (1): 82-90.
- 344 10. Sandrine D, Lucie S, Jean LC. Physico-chemical parameters that govern nanoparticles
345 fate also dictate rules for their molecular evolution. Adv Drug Deliver Rev. 2012; 64 (2):
346 179-89.
- 347 11. Zeng N, Gao X, Hu Q, Song Q, Xia H, Liu Z, et al. Lipid - based liquid crystalline
348 nanoparticles as oral drug delivery vehicles for poorly water - soluble drugs: cellular
349 interaction and *in vivo* absorption. Int J Nanomed. 2012; 7 (1): 3703-18.
- 350 12. Müller RH, Jacobs C. Kayser O. Nanosuspensions as particulate drug formulations in
351 therapy, rationale for development and what we can expect for the future. Adv Drug
352 Deliver Rev. 2001; 47 (1): 3-19.
- 353 13. Libo W, Jian Z, Wiwik W. Physical stability of nanoparticles. Adv Drug Deliver Rev.
354 2011; 63 (6): 456-69.

- 355 14. Lei G, Dianrui Z, Minghui C. Drug nanocrystals for the formulation of poorly soluble
356 drugs and its application as a potential drug delivery system. *J Nano Res.* 2008; 10 (5):
357 845-62.
- 358 15. Lei Y, Caixia L, Yua L, Jian FC, Haikui Z. Stabilized amorphous glibenclamide
359 nanoparticles by high gravity technique. *Mat Chem Phys.* 2011; 13 (1): 361-66.
- 360 16. Coppack SW, Lant AF, McIntosh CS. Pharmacokinetic and pharmacodynamic studies of
361 glibenclamide in non-insulin dependent diabetes mellitus. *Br J Clin Pharmacol.* 1990; 29
362 (6): 673- 84.
- 363 17. Dora CP, Singh SK, Kumar S, Datusalia AK, Deepa A. Development and
364 characterization of nanoparticles of glibenclamide by solvent displacement method. *Acta
365 Pharma Drug Res.* 2010; 67 (1): 283-90.
- 366 18. Elbary A, Salem HF, Maher ME. In vitro and in vivo evaluation of glibenclamide
367 using surface solid dispersion (SSD) approach. *Br J Pharmacol Toxicol.* 2011; 2
368 (1): 51-62.
- 369 19. Cornelia MK, Müller RH. Drug nanocrystals of poorly soluble drugs produced by
370 high pressure homogenization. *Eur J Pharm Biopharm.* 2006; 62 (1): 3-16.
- 371 20. Shasha R, Yunmei S, Frank P, Allan ME. Particle size reduction to the nanometer range a
372 promising approach to improve buccal absorption of poorly water soluble drugs. *Int J
373 Nano Med.* 2011; 6 (1):1245-51.
- 374 21. Sonke R, Albrecht S, Thomas R, Claudia SL. Thermal degradation of amorphous
375 glibenclamide. *Eur J Pharm Biopharm.* 2012; 83 (1): 76-86.

- 376 22. Corrosion Testing Laboratories. Corrosion Failure Analysis and Material Section
377 Specialists. Accessed 2013; April 10, 2013. Available from
378 <http://www.corrosionlab.com/facilities/ftir-interpretation.htm>
- 379 23. Heike B, Tobias U. Characterization of lipid nanoparticles by differential scanning
380 calorimetry, X-ray and neutron scattering. *Adv Drug Deliver Rev.* 2007; 59 (6): 379- 02.
- 381 24. Jane W, Sabine G, Heather O, Lakshmy N, Thomas G, Philip WG, et al.
382 Physicochemical stability of phospholipid-dispersed suspensions of crystalline
383 itraconazole. *Eur J Pharm Biopharm.* 2008; 69 (3): 1104-13.
- 384 25. Lai F, Sinico C, Ennas G, Marogiu F, Marogiu G, Fadda AM, et al. Dioclofenac
385 nanosuspensions: influence of preparation procedure and crystal form on drug dissolution
386 behaviour. *Int J Pharm.* 2009; 373 (1-2): 124-32.
- 387 26. Barrett ER. Nanosuspensions in drug delivery. *Nat Rev.* 2004; 3 (9): 785-96.
- 388 27. Bhaskar C, Shyam S, Anant P. Preparation and evaluation of glibenclamide polyglycolized
389 glyceride solid dispersions with silicon dioxide by spray drying technique. *Eur J Pharm*
390 *Sci.* 2005; 26 (2): 219-30.